Generation of monodisperse microemulsions in the colloidal range and stabilized monodisperse microbubbles with diameters of 5 microns using two different types of micro fluidic devices.

E. Castro-Hernández*, W. Van Hoeve**, F. Campo-Cortés*, D. Lohse** and J. M. Gordillo*

* Departamento de Ingeniería Aeroespacial y Mecánica de Fluidos, Universidad de Sevilla
Av. Descubrimientos s/n, 41092, Sevilla, Spain. Corr. author: jgordill@us.es.
** Department of Applied Physics, U. Twente, P.O. Box 217, 7500 AE Enschede, The Netherlands

ABSTRACT

Here we propose two different ways to generate either monodisperse microemulsions or monodisperse microbubbles. The first of these techniques, the coflow configuration, consists of a flow rate Q_i of a fluid with a viscosity μ_i that discharges into an immiscible liquid of viscosity μ_o that flows in parallel with the axis of the injector. When operating under the appropriate conditions, concentrated emulsions composed of micron-sized drops with a narrow size distribution can be generated. Nevertheless, this procedure is not equally valid to generate the type of monodisperse bubbles required in many different pharmaceutical, medical and material science applications. As a consequence, we propose a variant of the coflow configuration implemented in a two-dimensional PDMS device for the production of $\sim 5\,\mu\,m$ bubbles with a polydispersity index below 5% at high production rates ($> 10^5$ bubbles/s).

Keywords: microemulsions, bubbles, droplets, coflow, contrast agents

1 GENERATION OF MONODISPERSE MICROEMULSIONS IN THE COLLOIDAL RANGE BY MEANS OF A COFLOW OF TWO IMMISCIBLE STREAMS

When the outer capillary number verifies the condition $Ca_o = \mu_o U_o/\sigma \geqslant 5$, where U_o and σ indicate, respectively, the outer velocity and the interfacial tension coefficient and if the inner to outer velocity ratio is such that $U_i/U_o = Q_i/(\pi U_o R_i^2) \ll 1$, with R_i the inner radius of the injector, a jet is formed with the same type of cone-jet geometry predicted by the numerical results of [1]. For extremely low values of the velocity ratio U_i/U_o, we find that the diameter of the jet emanating from the tip of the cone is so small that drops with sizes below $1\,\mu\,m$ can be formed. We also show that, through this simple method, concentrated emulsions composed of micron-sized drops with a narrow size distribution can be generated.

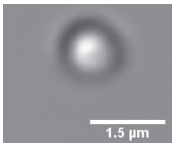

Figure 1: Image taken from Marín *et al.* Oil drop with a diameter smaller than $1\,\mu\,m$ obtained using glycerine and silicon oil of 10 cp as the outer and inner fluids respectively.

As it is described in [2], the tip streaming regime occurs under conditions such that the outer Reynolds number satisfies $Re_o = \rho_o U_o R_i/\mu_o \ll 1$, with ρ the liquid density. In addition, since viscous stresses need to overcome the interfacial tension confinement stresses to create the jet, the outer capillary number, defined here as $Ca_o = \mu_o U_o/\sigma$, must be larger than a certain constant of order unity. Consequently, in all the experimental results reported here, $Ca_o \geqslant 5$. Another necessary condition to observe the cone to jet transition is that $q \ll 1$, with q the velocity ratio $q = Q_i/(\pi R_i^2\, U_o) = U_i/U_o$. Finally, an inner Reynolds number such that $Re_i = \rho_i U_i R_i/\mu_i \ll 1$ ensures an efficient diffusion of the outer momentum across the jet section. Since both the inner and outer Reynolds numbers are much smaller than unity and the Bond number, defined here using the gravitational acceleration g as $Bo = |\rho_i - \rho_o| g R_i^2/\sigma$, also satisfies the condition $Bo \ll 1$, our experiments are controlled by only three dimensionless parameters [3], namely, the velocity ratio $q = Q_i/(\pi R_i^2 U_o)$, the viscosity ratio $\lambda = \mu_i/\mu_o$ and the capillary number $Ca_o = \mu_o U_o/\sigma$.

As it is described in [4], for fixed values of λ and Ca_o, the diameter of the liquid jet and, consequently, the diameter of the drops generated decrease when the velocity ratio is decreased. Interestingly enough, as it is shown in both [2] that, in the extreme limit $q \to 0$, drops with sizes below one micron can be generated through the simple procedure detailed here, as it is shown in figure 1.

Below a certain capillary number of order unity, drops are formed right at the tip of the injection needle [5]. Above this threshold, the most visible effect of increasing the capillary number when q and λ are kept constants is that the breakup length of the jet is approximately proportional to the capillary number, namely, $l_b = L_b/R_i \propto Ca_o$. The cone to jet transition region becomes more slender as the capillary number decreases. Nevertheless, far downstream the exit of the tube neither the diameter of the jet nor the diameter of the drops generated vary significatively with Ca_o.
When the viscosity ratio, λ, decreases keeping both q and Ca_o constant, the cone to jet transition region becomes more elongated, the jet is stable and breaks into drops periodically. However, for values of the viscosity ratio below a certain threshold, the jet is no longer stable and drops are formed in a non periodic way.

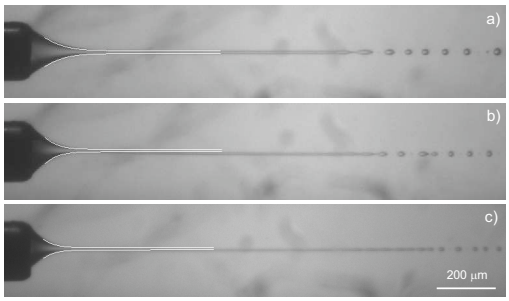

Figure 2: Image taken from Castro-Hernández *et al.* (2012). Experimental images obtained using silicon oil of 10 cp as the inner fluid and glycerine as the outer ($\lambda = 10^{-2}$). The continuous white line indicates the theoretical jet shape obtained integrating the third order differential equation. The values of the control parameters in each of the three cases shown are: (a) $Ca_o = 5$, $q = 10^{-2}$, $Q_i = 5 \times 10^{-1}\,\mu l/min$, $Q_o = 7\,ml/min$; (b) $Ca_o = 9$, $q = 6 \times 10^{-3}$, $Q_i = 4 \times 10^{-1}\,\mu l/min$, $Q_o = 12\,ml/min$; (c) $Ca_o = 12$, $q = 5 \times 10^{-3}$, $Q_i = 5 \times 10^{-1}\,\mu l/min$, $Q_o = 16\,ml/min$.

Thanks to the information extracted from numerical simulations of boundary-integral type and using the slender-body approximation due to [6], we deduce a third-order, ordinary differential equation that predicts, for arbitrary values of the three dimensionless numbers that control this physical situation, namely, Ca_o, μ_i/μ_o and U_i/U_o, the shape of the jet and the sizes of the drops generated. Most interestingly, the influence of the geometry of the injector system on the jet shape and drop size [7] enters explicitly into the third-order differential equation through two functions that can be easily calculated numerically. As it is depicted in figures 2 and 3, our theory is capable to predict the cone-jet geometry of

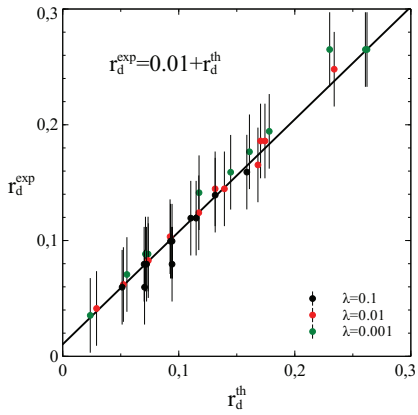

Figure 3: Comparison of the theoretical drop size, r_d^{th} with experiments. The experimental error bars are calculated assuming that there is an uncertainty of 1 pixel (1.45 $\mu\,m$) in the measurement of the experimental drop radius, r_d^{exp}.

the liquid thread formed as well as the size of the drops generated. This theoretical description can also be used as an efficient tool for the design of new emulsification devices.

From the point of view of applications, the simple coflow configuration operated in the tip streaming regime is an efficient method for the production of concentrated micro-emulsions composed of drops with a narrow size distribution, as it is depicted in figure 4. Indeed, since the formation process is periodic when the inner fluid is a liquid instead of a gas, drop size can be fixed with great accuracy by controlling q, λ and Ca_o, as shown in figure 3. Nevertheless, since the bubble formation process is not periodic, this procedure is not equally valid to generate the type of monodisperse bubbles required in many different pharmaceutical, medical and material science applications. Other techniques, such as that described in the next section, are more adequate for such purposes.

2 GENERATION OF STABILIZED MONODISPERSE MICROBUBBLES WITH DIAMETERS OF 5 MICRONS IN PDMS DEVICES WITH A FLOW FOCUSING GEOMETRY

Here we describe a new method for the controlled production of $\sim 5\,\mu\,m$ bubbles with a polydispersity index below 5% at high production rates ($> 10^5$ bubbles/s) by means of a planar flow focusing device [8].

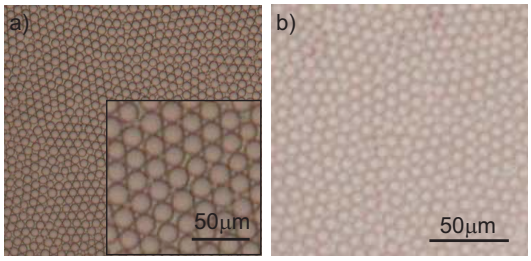

Figure 4: Image taken from Castro-Hernández *et al.* (2012).Concentrated emulsions using silicon oil with a viscosity of $10\,cp$ as the inner fluid and a $16\,mM$ SDS (Sodium Dodecyl Sulfate) glycerine and water mixture with a viscosity of $100\,cp$ as the outer one. Here, $\sigma = 55\,mN/m$. (a) $D_d = 19\,\mu m$, $Ca_o = 5 \times 10^{-1}$, $q = 7 \times 10^{-2}$, $Q_i = 6\,\mu l/min$, $Q_o = 10\,ml/min$. The inset shows the crystal-like structure of the resulting emulsion; (b) $D_d = 8\,\mu m$, $Ca_o = 5 \times 10^{-1}$, $q = 8 \times 10^{-3}$, $Q_i = 1\,\mu l/min$, $Q_o = 10\,ml/min$. Concentrated emulsions composed of drops with sizes close to $1\ \mu m$ can be also generated. Nevertheless, due to the smallness of these drops, the images corresponding to these types of emulsions appear blurred and thus, are not shown here.

The essential geometrical difference of our device with respect to *all* previous implementations is that the length of the exit channel L is much larger than its width namely, $L/w \gg 1$, as depicted in figure 5. This, together with the fact that the imposed liquid and gas flow rates, Q_g and Q_l respectively, are such that $Re \gtrsim 10^2$, $We \gg 1$ and $Q_g/Q_l \ll 1$, enables the production of bubbles in water with sizes one order of magnitude smaller than the channel width. In this way, we are able to produce, in a single step, bubbles with sizes within the range needed for therapeutical applications avoiding clogging problems. The bubble size can be predicted based on the gas to liquid flow rate ratio and the fluid properties as

$$d_b/w \simeq 2.75(\mu_g/\mu_l)^{1/12}(Q_g/Q_l)^{5/12}\,, \qquad (1)$$

with μ_g and μ_l the gas and liquid viscosities respectively.

Figure 5 shows a global view of the microchannel entrance region, which is where microbubbles are formed thanks to a strong pressure gradient. The figure reveals that – thanks to our choice $Q_g/Q_l < 0.03$ – the gas filament contracts from the width of the gas supply channel ($400\,\mu m$) to a steady ligament whose diameter is substantially smaller than w. Due to the fact that the height (h) of the device is equal to the width of the exit channel ($h = w \gg d_b$), the gas thread separates from the lower glass surface at the region indicated as *detachment line*. Indeed, since the PDMS substrate is less hydrophilic than the glass one ($\theta_{\rm PDMS} \simeq 90°$ and

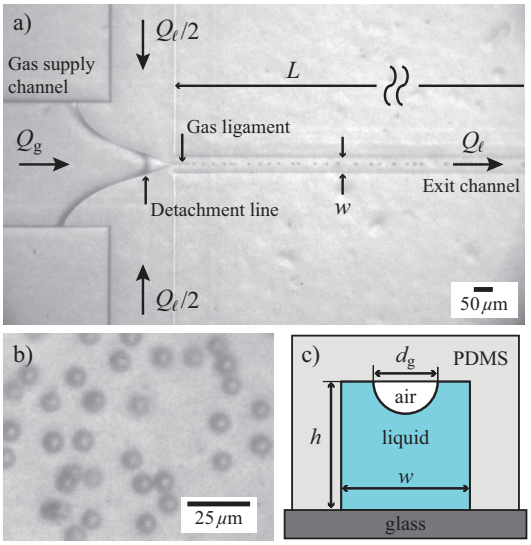

Figure 5: Image taken from Castro-Hernández *et al.* (2011).(a) High speed photograph showing the formation of microbubbles using our microfluidic flow-focusing geometry, $w = 50\,\mu m$, $L/w = 30$. The outer liquid flow forces the inner gas flow to form a tiny gas ligament that detaches from the channel wall and breaks up into microbubbles. The size of the microbubbles $d_b = 7.2\,\mu m$ is much smaller than the channel width. The gas and liquid pressures are $p_g = 1555\,\mathrm{mbar}$ and $p_l = 1597\,\mathrm{mbar}$ respectively, being the liquid flow rate $U_l = 7.67\,\mathrm{m\,s^{-1}}$. (b) Microbubbles immediately after exiting the channel. (c) Schematic representation of a cross-section of the microfluidic channel downstream the detachment line. The gaseous ligament dewets the PDMS channel wall.

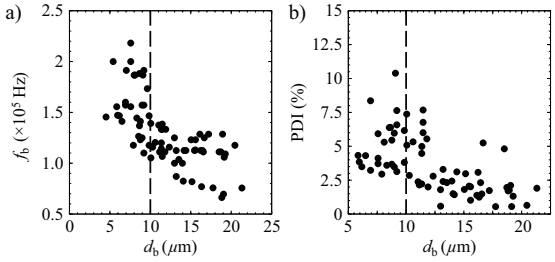

Figure 6: (a) Bubble formation frequencies as a function of bubble diameter. Note that all bubbles with diameters below $10\ \mu m$ are produced at frequencies that exceed 10^5 Hz. (b) PDI index, in %, as a function of bubble diameter. Note that, for many experimental conditions, bubbles with diameters $d_b \simeq 5\ \mu m$ can be produced with values of the PDI index below 5%. The reason for which the PDI index is larger for some experiments is attributable to the fact that some images are out of the focus plane and are a bit blurred.

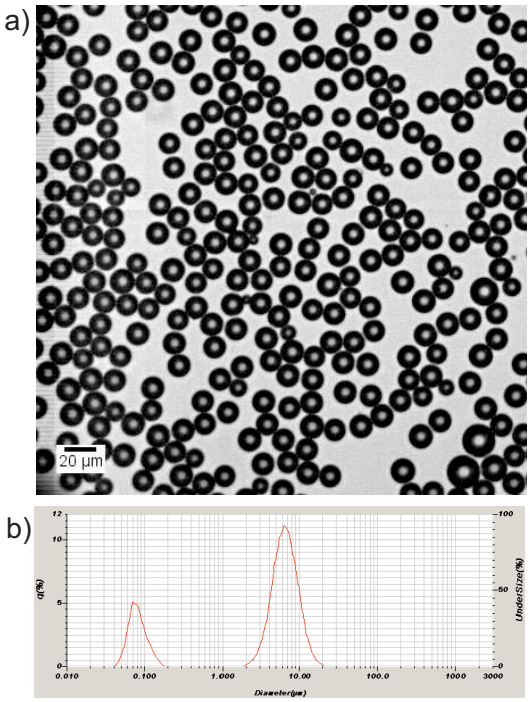

Figure 7: (a) This figure shows the type of phospholipid-covered bubble dispersion in a liquid at the moment of generation. In (b), the size distribution of the same bubble dispersion depicted in (a) measured after three days through a coulter-counter. The peak observed in the range of sizes below 1 $\mu\,m$, is attributed to the formation of phospholipid micelles.

$\theta_{\text{glass}} = 39.5°$) the narrow gas ligament, of diameter $d_g \ll w$, is attached to the upper PDMS surface. Once the steady gas ligament is formed, it breaks into uniformly sized bubbles with diameters $db \sim d_g \sim 5\mu\,m$ which, as depicted in figure 6, can be produced at frequencies exceeding $10^5\ Hz$ with values of the polydispersity index (PDI) below 5%

As a particularly important application, in figure 7, we show that our procedure is able to generate monodisperse bubbles with a phospholipid cover [9] that prevents their dissolution and with diameters, $d_b \simeq 5\,\mu\,m$, which are in the range of sizes required in therapeutical or cleaning technology applications.

REFERENCES

[1] Suryo, R. & Basaran, O. A., Tip streaming from a liquid drop forming from a tube in a co-flowing outer fluid. *Phys. Fluids*, Volume 18, 082102 (2006)

[2] Marín, A. G. & Campo-Cortés, F. & Gordillo, J. M., Generation of micron-sized drops and bubbles through viscous coflows. *Colloids Surf. A: Physicochem. Eng. Aspects*, Volume 344, 2 – 7 (2009)

[3] Castro-Hernández, E. & Gundabala, V. & Fernández-Nieves, A. & Gordillo, J. M. , Scaling the drop size in coflow experiments. *New J. Phys.*, Volume 11, (2009)

[4] Castro-Hernández, E. & Campo-Cortés, F.& Gordillo, J. M., Slender-body theory for the generation of micrometre-sized emulsions through tip streaming. *J. Fluid Mech.*, doi:10.1017, (2012)

[5] Utada, A. S. & Fernández-Nieves, S. & Stone, H. A. & Weitz, D., Dripping to jetting transitions in co-flowing liquid streams. *Phys. Rev. Lett.*, Volume 99, 094502 (2007)

[6] Taylor, G. I., Conical free surfaces and fluid interfaces. *Proceedings of the 11th International Congress of Applied Mechanics*, 790 – 796 (1964)

[7] Tomotika, S., On the Instability of a Cylindrical Thread of a Viscous Liquid Surrounded by Another Viscous Fluid. *Proc. Roy. Soc.*, Volume 150, 322 – 337 (1935)

[8] Castro-Hernández, E. & Van Hoeve, W. & Lohse, D. & Gordillo, J. M., Microbubble generation in a co-flow device operated in a new regime. *Lab On a Chip*, Volume 11, 2023 – 2029 (2011)

[9] Hettiarachchi, K. & Talu, E. & Longo, M. L. & Dayton, P. A & Lee, A. P., On-chip generation of microbubbles as a practical technology for manufacturing contrast agents for ultrasonic imaging. *Lab On a Chip*, Volume 7, 463–468 (2007)